清洁能源科学与技术 第 1 卷 第 2 期（2023）
Journal of Clean Energy Science and Technology Volume 1 Issue 2 (2023) doi: 10.18686/cncest.v1i2.91

综述文章

含有纳米碳填料的3D打印可拉伸导电聚合物复合材料的多功能应用

赵晨鹏†, 李汝晴†, 方彪, 王睿, 梁晗, 王磊, 吴瑞林, 韦愈楠, 王璋元, 粟志鹏, 莫润伟*

机械与动力工程学院，华东理工大学，上海 200231，中国

*** 通讯作者：**莫润伟，rwmo@ecust.edu.cn

† 赵晨鹏和李汝晴对本文的贡献相同。

摘要：碳纳米材料因其稳定性好、导电性强、价格低廉而被广泛用作基底材料来制备可拉伸导电复合材料。针对优化复合材料性能的需求，各种制备碳纳米材料增强可拉伸导电复合材料的制造方法应运而生。其中，3D 打印技术具有工艺灵活、产品性能优良等优点，受到广泛关注。本文重点综述利用 3D 打印技术在高分子材料中添加碳纳米材料作为增强相的研究进展。 展望了基于纳米碳填料的导电聚合物复合材料在航空航天、储能、生物医学等领域的应用前景。

关键词：碳基材料；3D 打印技术；聚合物复合材料；结构设计；电子设备

1. 前言

基于纳米碳填料制备的可拉伸导电复合材料是指以碳材料作为导电填料的复合材料。可拉伸导电复合材料的关键在于需要在大应变下保持导电网络，并在应变释放后恢复其原有特性。一般来说，柔性和弹性聚合物具有出色的拉伸性能，但导电性能较差[1–4]。虽然石墨烯、碳纳米管（carbon nanotubes, CNT）和炭黑（carbon black, CB）等碳纳米材料具有较高的导电性[5]，但它们的拉伸性能较差[6,7]。因此，通常将纳米导电材料与可拉伸聚合物以特定方式混合，制备可拉伸导电纳米复合材料，应用于可拉伸电池、应变传感器、可拉伸超级电容器和可穿戴医疗设备等领域[8,9]。值得注意的是，与金属导电填料相比，碳材料具有更好的稳定性和改性能力，重量更轻，价格更低，因此可以实现大规模生产，以满足对新型电子设备日益增长的需求[10–18]。

近年来，3D 打印技术发展非常迅速，已广泛应用于航空航天、生物医学、能源存储等多个领域[19–26]。它被认为是一种很有前途的新型制造成型技术[27]。3D 打印技术也为聚合物基复合材料的制备提供了新思路[28,29]。将 3D 打印技术与碳纳米材料/聚合物基复合材料的制备相结合，可以实现复合材料的快速制造[30–32]。这为复杂结构产品的制造提供了一条新途径。碳纳米材料的添加使得 3D 打印产品具有更好的力学性能、电学性能和功能特性，也更方便制备梯度功能产品[33,34]。此外，3D 打印的逐层制造方法抑制了碳纳米材料在聚合物基体中的大面积团聚，更有利于实现均匀分散[35]。如**图 1** 所示，3D 打印的纳米碳填料可拉伸导电聚合物复合材料表现出良好的机械和电学性能，在电子、航空航天、储能和生物医学等领域显示出巨大的应用潜力。本文介绍了 3D 打印形成碳纳米材料/聚合物基复合材料的研究，简要介绍了碳纳米材料/聚合物基复合材料的制备方法，总结了 3D 打印工艺及应用领域。

收稿日期：2023-11-07 录用日期：2023-11-20 发表日期：2023-11-24
版权 © 2023 作者。《清洁能源科学与技术》由 Universe Scientific Publishing 出版。本文是一篇开放获取文章，使用知识共享署名—非商业性使用 4.0 国际许可协议（Creative Commons Attribution-NonCommercial 4.0 International License, http://creativecommons.org/licenses/by-nc/4.0/），允许第三方用户进行自由共享（即用任何媒介以任何形式复制、发行原文）、演绎（即修改、转换或以原文为基础进行创作），但必须适当引用原文。
English edition of this article is available online at https://cae.usp-pl.com/index.php/cest/article/view/84

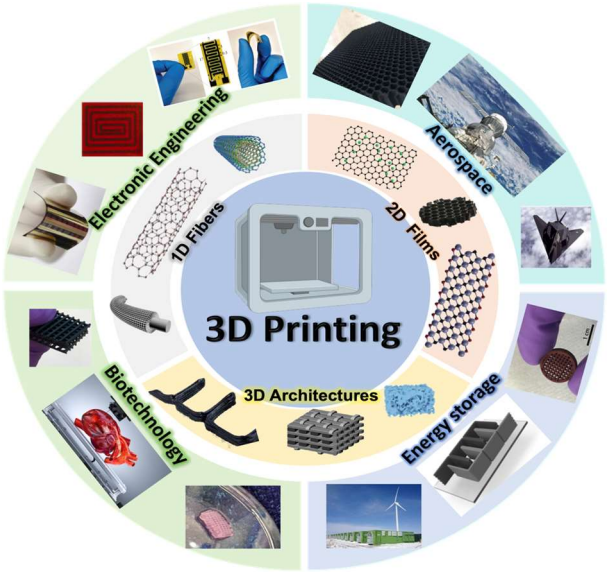

图 1. 含有纳米碳填料的三维打印可拉伸导电聚合物复合材料及其应用示意图。
Figure 1. A scheme of 3D-printed stretchable conductive polymer composites with nano-carbon fillers and their applications.

2. 碳基聚合物复合材料的分类

碳材料因其价格低廉、稳定性好、原料储备丰富、生物相容性好等优点，成为目前应用最广泛的材料之一[36]。主要包括石墨、碳纤维、炭黑、石墨烯、石墨炔、碳纳米管、富勒烯（C_{60}）等。石墨是最常见的碳材料，常用于耐腐蚀材料、润滑材料、耐火材料以及制备氧化石墨烯的原料[37]。碳纤维是一种主要由碳元素组成的特种纤维[38]。它具有优异的沿纤维轴的机械强度和模量。因此，常被用作增强材料与聚合物、金属或陶瓷结合制备复合材料。C_{60} 是一种完全由碳组成的新型中空分子。目前，它在有机太阳能电池领域多用作电子传输层，可以提高电池的光电转换效率[39]。而炭黑、石墨烯、碳纳米管尺寸较小，电性能优异，属于纳米级导电材料。因此，它广泛应用于可拉伸导电纳米复合材料。

2.1. 炭黑

作为最重要的碳基填料之一，炭黑已被广泛应用于各种工业生产中。这种纳米材料具有比表面积大、化学稳定性好、导电导热性高、成本低等一系列优点。炭黑主要由碳氢化合物热分解或不完全燃烧产生。炭黑颗粒的大小、结构和导电性在很大程度上取决于原材料的选择和制造方法。炭黑颗粒具有无定形和准石墨结构，平均粒径为 3–100 nm。值得注意的是，炭黑颗粒往往会团聚在一起形成聚集体，这些聚集体在范德华力的作用下会形成更大的空间网络结构聚集体。 因此，如何避免炭黑颗粒团聚是研究的重点和难点。最近，Bhagavatheswaran 等[40]通过混合炭黑和丁苯橡胶成功制备了复合材料，如**图 2(a–c)**所示。值得注意的是，研究人员通过添加二氧化硅颗粒来阻止炭黑的团聚。结果表明，该复合材料的电导率为 40 S m^{-1}，最大拉伸率为 200%，并探索了其在压力传感器中的应用。Niu 等[41]利用炭黑和聚二甲基硅氧烷成功制备了可拉伸导电复合材料，如**图 2(d–f)**所示。研究结果表明，该复合材料具有良好的导电性和机械稳定性，可用于组装生物微芯片。此外，Song 等[42]利用炭黑和碳纳米管与聚己二酸/对苯二甲酸丁二醇酯（polybutylene adipate/terephthalate, PBAT）混合制备复合材料，将其用作水系锂离子电池的集流体，如**图 2(g–i)**所示。研究结果表明，在 100%应变下仍能正常工作，且添加碳纳米管后复合材料的导电性能得到显著提高。

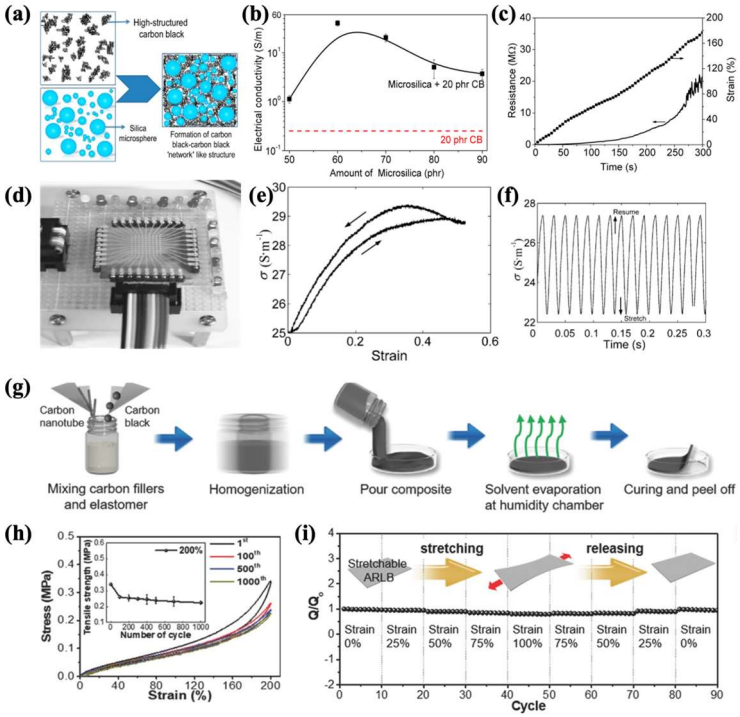

图 2. (a) 导电炭黑颗粒的强填料—填料网络的开发。**(b)** 不同微硅含量的混合复合材料的电阻图。**(c)** 应变阻力[40]。**(d)** 使用 LED 测试电路以显示粘合板的功能。**(e)** 炭黑粉末和 PDMS（CPDMS）以 1.5 mm min^{-1} 的速率进行准静态拉伸和恢复。**(f)** CPDMS 样品的动态拉伸特性，峰峰值幅度 1 mm，50 Hz[41]。**(g)** 碳/聚合物复合材料的制造步骤。**(h)** 包含杂化碳/聚合物复合材料的可拉伸电极在 200%应变下的疲劳测试，重复 1000 个循环。插图显示了电极的拉伸强度与应变循环次数的关系，最大值为 1000 次。**(i)** 可拉伸水性可充电锂离子电池在不同应变量下的相对放电容量[42]。

Figure 2. (a) Development of a strong filler—filler network of the conducting carbon black particle. **(b)** Plot of electrical resistance for hybrid composites with different microsilica contents. **(c)** Resistance with strain[40]. **(d)** Testing the circuit with LEDs to show the functionality of the bonded plate. **(e)** Quasi-static stretching and restoring at a rate of 1.5 mm min^{-1} for carbon black powder and PDMS (CPDMS). **(f)** Dynamic stretching characteristics of the CPDMS sample, peak-to-peak amplitude 1 mm, 50 Hz[41]. **(g)** Steps for the fabrication of the carbon/polymer composite. **(h)** Fatigue test of the stretchable electrode containing the hybrid carbon/polymer composite under a strain of 200% that was repeated for 1000 cycles. The inset shows the tensile strength of the electrode as a function of the number of strain cycles, with the maximum value being 1000 cycles. **(i)** The relative discharge capacity of the stretchable aqueous rechargeable lithium-ion battery under various amounts of strain[42].

2.2. 碳纳米管

从晶体结构分析，碳纳米管是由石墨烯片（六边形结构）按特定螺旋角度卷曲而成的空心圆柱管状结构。碳纳米管有两种类型：（1）单壁碳纳米管（single-walled carbon nanotubes, SWCNTs），可以看作是单个石墨烯片卷成的圆柱体。（2）多壁碳纳米管（Multi-walled carbon nanotubes, MWCNTs），可以看作是多个同心层石墨烯的堆叠。制备碳纳米管的方法很多，主要包括激光烧蚀、电弧蒸发、化学气相沉积（chemical vapor deposition, CVD）等。碳纳米管具有高模量、高刚度、高导电性和低密度等特点，是制备复合材料的理想材料。最近，Shin 等[43]使用化学气相沉积获得的 MWCNT 与聚氨酯混合制备了复合材料。值得注意的是，如**图 3(a,b)**所示，在 10%–20%的应变范围内，复合材料的导电性几乎没有下降。Sekitani 等[44]通过混合单壁碳纳米管和含氟橡胶制备了复合材料，如**图 3(c–e)**所示。制备的复合材料具有大于 100 S cm^{-1} 的导电性和超过 100%的拉伸性。基于这种复合材料，成功构建了一种可拉伸的有源矩阵显示屏。Liu 等[45]使用还原氧化石墨烯（reduced graphene oxide, rGO）和碳纳米管作为导电填料，丁苯橡胶作为聚合物制备了一种复合材料，如**图 3(f,g)**所示。研究结果表明，复合材料的导电率达到了 3.62 S cm^{-1}，并能在低拉伸应变下保持稳定。更重要的是，与炭黑导电纳米复合材料相比，其性能有了显著提高。

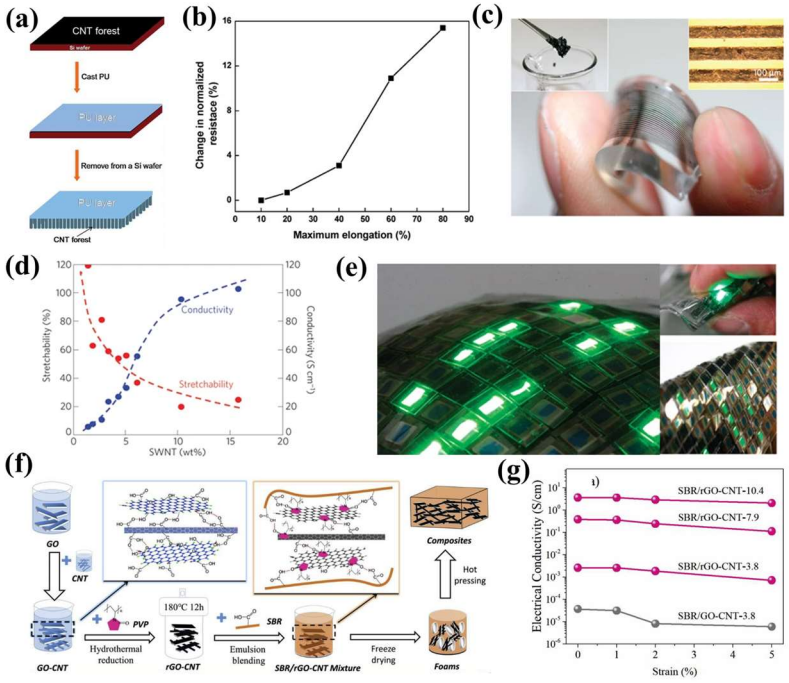

图 3. (a) 森林/聚氨酯复合片材的制备方法示意图。**(b)** 图中显示的从第 10 个循环到第 100 个循环的归一化电阻变化与最大应变的函数关系。每个应变组的前 10 个循环用于提供初始样品调节[43]。**(c)** 印刷在 PDMS 片材上的弹性导体。**(d)** 拉伸性和导电性与 SWCNT 含量的函数关系。**(e)** 可在任意弯曲表面上铺展的可拉伸显示屏演示。这种可拉伸显示屏即使折成两半或揉成一团也能正常工作，显示出卓越的耐用性[44]。**(f)** rGO-CNT 混合材料和丁苯橡胶/rGO-CNT 复合材料的制备示意图。**(g)** 不同应变下 SBR/GO-CNT 和 SBR/rGO-CNT 复合材料导电率的变化[45]。

Figure 3. (a) Schematic diagram of the preparation method for the forest/polyurethane composite sheet. **(b)** Change in normalized resistance shown in the graph in going from the 10th to the 100th cycle as a function of the maximum applied strain. The first 10 cycles for each strain set were used to provide initial sample conditioning[43]. **(c)** Printed elastic conductors on a PDMS sheet. **(d)** Stretchability and conductivity as a function of SWCNT content. **(e)** A demonstration of a stretchable display that can be spread over arbitrary curved surfaces. The stretchable display is functional even when folded in two or crumpled, indicating excellent durability[44]. **(f)** Schematic illustration for preparation of rGO-CNT hybrid and styrene-butadiene rubber (SBR)/rGO-CNT composites. **(g)** Changes in electrical conductivity of SBR/GO-CNT and SBR/rGO-CNT composites under different strains[45].

2.3. 石墨烯

石墨烯由单层碳原子组成，呈二维蜂窝状晶格排列，可通过变形获得其他碳材料。石墨烯具有许多优异特性，如高比表面积、高导电性和电子迁移率、优异的热稳定性和化学稳定性以及机械柔韧性[46]。此外，石墨烯还可以通过界面改性的方法获得多种衍生物。例如，掺杂元素的石墨烯是构建自支撑石墨烯复合材料的基础，这种复合材料具有优异的机械、电气和热性能。最近，Chen 等[47]通过化学气相沉积法制备了具有三维结构的石墨烯，并将其填充到聚二甲基硅氧烷中制备了一种复合材料，如**图 4(a–c)**所示。这种复合材料具有优异的导电性，可作为可拉伸导体应用于各个领域。Wang 等[48]利用石墨烯泡沫和聚二甲基硅氧烷制备了一种可拉伸的石墨烯蜂窝复合结构，如**图 4(d–g)**所示。该复合材料的电导率为 72 S m^{-1}。值得注意的是，利用这种材料作为电路，成功制造出了可拉伸的发光显示器。此外，Sun 等[49]利用石墨烯和聚氨酯纤维制备了可拉伸导电纤维，可用于应变传感器和可拉伸导体，如**图 4(h–k)**所示。然而，三维结构石墨烯与聚合物的渗透过程通常比较复杂，不利于大规模制备。

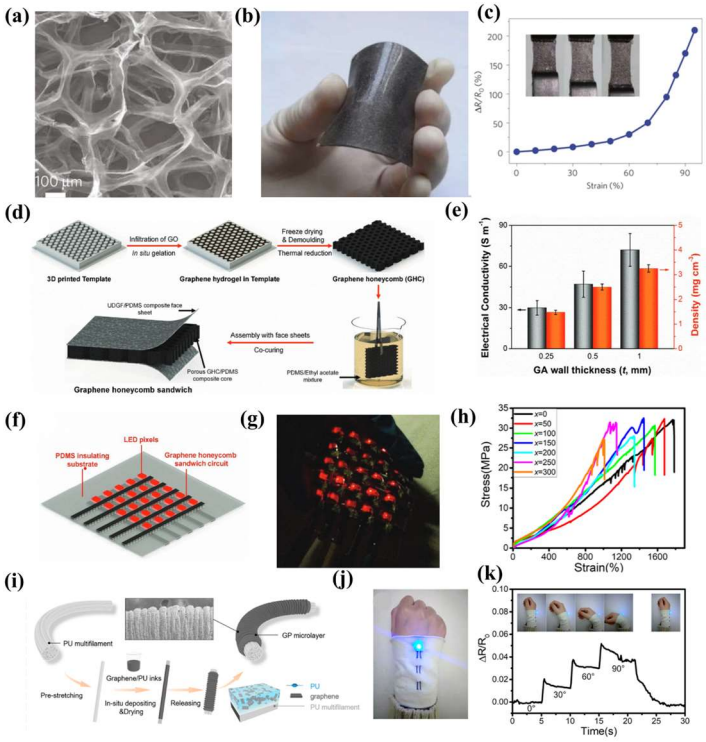

图 4. (a) 石墨烯泡沫（graphene foam, GF）的 SEM 图像。**(b)** 弯曲 GF/PDMS 复合材料的照片，显示其具有良好的柔韧性。**(c)** GF 和 GF/PDMS 复合材料的导电率与石墨烯层数的函数关系[47]。**(d)** 制作 GHC 和 GHC 夹层。**(e)** *t* 为 0.25 至 1 mm 的石墨烯蜂窝（Graphene honeycomb, GHC）。**(f)** 使用 GHC 夹层构建的可拉伸发光显示器示意图。**(g)** 可拉伸发光显示器的照片[48]。**(h)** 制作虫形丝的示意图。**(i)** 传导率–应变曲线。**(j)** 应变敏感拉伸电子器件的潜在应用。**(k)** 编织在织物中的丝线可在手腕关节运动时传导信号[49]。

Figure 4. (a) SEM image of graphene foam (GF). **(b)** A photograph of a bent GF/PDMS composite, showing its good flexibility. **(c)** Electrical conductivity of GFs and GF/PDMS composites as a function of the number of graphene layers[47]. **(d)** Fabrication of GHCs and GHC sandwiches. **(e)** Graphene honeycomb (GHC) with *t* ranging from 0.25 to 1 mm. **(f)** Schematic of a stretchable light-emitting display constructed using a GHC sandwich. **(g)** Photographs of the stretchable light-emitting display[48]. **(h)** Schematic diagram of preparing the worm-shaped filaments. **(i)** Conductivity-strain curves. **(j)** Potential applications of strain-insensitive stretchy electronics. **(k)** Filament woven into fabric to conduct signals under wrist joint movements[49].

近年来，研究人员通过添加碳纳米材料提高了可拉伸导电复合材料的性能。然而，仍有一些问题需要解决。最关键的方面是如何实现碳纳米材料在聚合物基体中的均匀分散。值得注意的是，碳纳米材料在聚合物中的分散程度极大地影响复合材料的综合性能。因此，为了充分利用碳纳米材料优异的力学和电学性能，需要开发新的机制、方法和技术来实现碳纳米材料在聚合物中的均匀分散。

3. 碳基聚合物复合材料的 3D 打印工艺

随着 3D 打印技术的不断发展和完善，各种新型 3D 打印技术层出不穷。近年来，利用 3D 打印技术制备碳基聚合物复合材料发展迅速[50]。目前，适用于碳基聚合物复合材料的 3D 打印工艺主要包括熔融沉积成型、喷墨打印、立体光刻设备和选择性激光烧结等。不同的印刷工艺有相应的优缺点，需要根据印刷材料的特性、工艺特点、产品用途综合选择。

3.1. 熔融沉积建模

熔融沉积建模（fused deposition modeling, FDM）主要适用于热塑性聚合物的三维打印，是目前最常用的三维打印方法。具体来说，这种方法需要将聚合物制备成标准直径的线材，然后通过步进电机将线材输送到喷嘴，加热并熔化后挤出。最后，在基底上按所需形状堆叠并粘合各层，冷却凝

固后即可获得所需的成型[51,52]。碳基聚合物基复合材料的熔融沉积成型可以通过将熔融混合、溶液混合等方法制备的碳基聚合物基复合材料制成 3D 打印线材来实现。纳米碳材料的加入不仅能提高复合材料的机械性能，还能赋予复合材料优异的电性能、热性能、摩擦性能和耐磨性能。

值得注意的是，丙烯腈-丁二烯-苯乙烯共聚物（acrylonitrile-butadiene-styrene copolymers, ABS）和聚乳酸（polylactic acid, PLA）是 FDM 最常用的聚合物。最近，Wei 等[53]通过将聚合物与氧化石墨烯（graphene oxide, GO）进行溶液混合，并加入水合肼进行还原，制备了 rGO/ABS 和 rGO/PLA 复合材料，拉丝后用于熔融沉积成型，如**图 5(a–d)**所示。研究结果表明，GO 的最大添加量可达 5.6%（质量分数，下同），导电率可达 1.05 × 10^{-3} S m^{-1}。碳纳米材料的加入会提高聚合物的玻璃化转变温度（Tg），因此与纯树脂相比，3D 打印温度需要适当提高。Zhu 等[54]将 6%的石墨烯纳米片（graphene nanosheets, GNPs）与尼龙 12（PA12）混合用于熔融沉积成型，如**图 5(e–j)**所示。结果表明，GNPs 在从喷嘴挤出的过程中会发生取向，与压缩成型相比，复合材料沿取向方向的热导率和弹性模量分别提高了 51.4%和 7%。熔融沉积建模不仅具有打印材料范围广、操作简单、设备成本低、操作方便、打印速度快等优点，而且可以用多个喷嘴同时打印不同类型的材料。因此，它是最具工业应用前景的打印方法之一。然而，这种方法也有不足之处，包括印刷精度不够、喷嘴堵塞、热应力不均匀、层间强度低等。

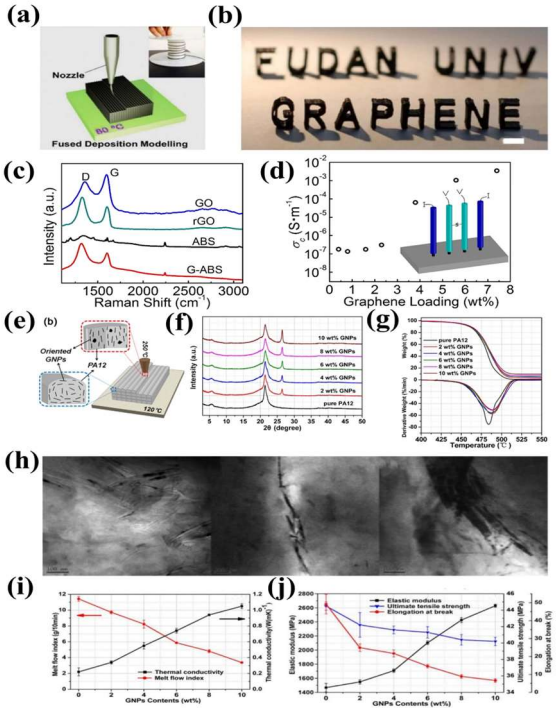

图 5. (a) 三维打印过程中熔融沉积建模的示意图。内图为石墨烯基长丝缠绕在滚筒上。**(b)** 使用 3.8 wt% G-ABS 复合长丝打印的典型 3D 模型，比例尺为 1 cm。**(c)** 制备的 GO、rGO、ABS 和 G-ABS 样品的代表性拉曼光谱。**(d)** G-ABS 复合材料的电导率（σ_c）与石墨烯负载的函数关系。插图是用于测量 σ_c 的四探针示意装置[53]。**(e)** 在 FDM 过程中，GNPs 在 PA12 基体中的取向。**(f)** PA12 和 PA12/GNPs 纳米复合材料与 2、4、6、8 和 10 wt% GNPs 压缩成型样品（10 mm × 10 mm × 4 mm）的 XRD 光谱。**(g)** 纯 PA12 和含有 2、4、6、8 和 10 wt % GNPs 的 PA12/GNPs 纳米复合材料的 TG（上）和 DTG（下）曲线。**(h)** PA12/6 wt% GNPs 纳米复合材料的 TEM 显微照片。**(i)** MFI 值、热导率（λ）。**(j)** 纯 PA12 和 PA12/GNPs 纳米复合材料及其 CM 试样的拉伸测试结果[54]。

Figure 5. (a) Schematic illustration of fused deposition modeling in the 3D printing process. Inset is the graphene-based filament winding on a roller. The filament was deposited through a nozzle onto a heated building plate, whose temperature was set at 80 ℃. **(b)** A typical 3D-printed model using 3.8 wt% G-ABS composite filament, scale bar: 1 cm. **(c)** Representative Raman spectra in prepared GO, rGO, ABS and G-ABS samples. **(d)** Electrical conductivity (σ_c) of G-ABS composites as a function of graphene loading. Inset is the four-probe schematic setup used in the σ_c measurement[53]. **(e)** Orientation of GNPs in the PA12 matrix during

the FDM process. **(f)** XRD spectra of PA12 and PA12/GNPs nanocomposites with 2, 4, 6, 8, and 10 wt% GNPs compression-molded samples (10 mm × 10 mm × 4 mm). **(g)** TG (top) and DTG (bottom) curves of pure PA12 and PA12/GNPs nanocomposites with 2, 4, 6, 8, and 10 wt % GNPs. **(h)** TEM micrographs of PA12/6 wt% GNPs nanocomposites. **(i)** The MFI values, thermal conductivity (λ). **(j)** Tensile test results of pure PA12 and PA12/GNPs nanocomposites and their CM specimens, respectively[54].

3.2. 喷墨打印

喷墨打印（Inkjet）已从最初仅用于文字和图片打印的技术发展成为一种快速原型制作方法。作为一种快速成型技术，它已广泛应用于电子电路、柔性设备等领域[55]。在常用的压电喷墨打印工艺中，打印材料首先溶解或分散在溶剂中形成“墨水”。然后，根据印刷需要，在压电陶瓷片上施加电压使其变形，空腔中的墨水受到挤压被一滴一滴地喷射出来，并在基板上一层一层地累积，形成要印刷的形状。最后，通过热处理、冷冻干燥等后处理方法去除溶剂凝固[56]。碳纳米材料的高载流子迁移率使其非常适合用于恢复纳米电子器件的导电性，使柔性材料具有优异的导电性和介电性能。喷墨打印是一种常用、便捷、高效的制备方法。添加聚合物可以稳定墨水，防止碳纳米材料沉淀和分层，还可以调节墨水的粘度，使其在方便打印的范围内。值得一提的是，为了调节油墨的粘度，研究人员发现可以在油墨中添加聚乙烯吡咯烷酮（polyvinylpyrrolidone, PVP）和乙基纤维素（ethyl cellulose, EC）作为稳定剂和粘度调节剂。

最近，Lim 等[57]将 GO 和聚乙烯醇（polyvinyl alcohol, PVA）溶于水并混合，然后用水合肼还原，制备出 rGO/PVA 墨水，如**图 6(a–g)**所示。最后，通过喷墨印刷制备出有机场效应晶体管的电极。结果表明，与传统的金电极和 PEDOT:PSS 电极相比，喷墨印刷的 rGO/PVA 电极的场效应迁移率有了很大提高。García-Tuñon 等[58]在氧化石墨烯片上接枝聚合物，制备 pH 响应型表面活性剂。研究结果表明，可以通过改变 pH 值来调节所得墨水的粘度，最后通过 100 μm 的喷嘴实现三维成型物体的连续打印，如**图 6(h–j)**所示。喷墨打印具有设备简单、操作方便、成本低廉等优点。因此，它非常适合制备微纳器件和电子电路。但是，这种方法也存在一些缺陷，包括制备的器件强度低、后处理后存在一些缺陷、器件从基底上脱落等。

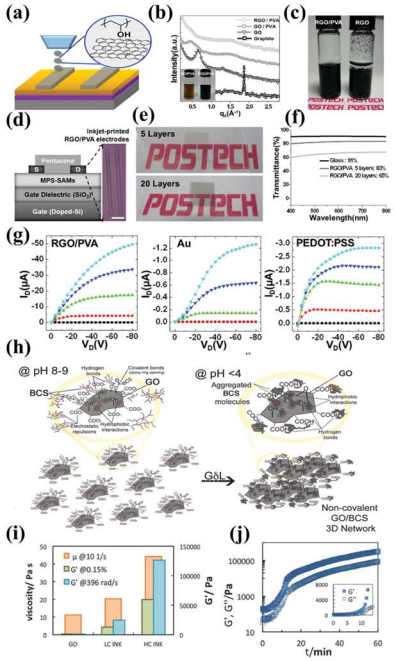

图 6. (a) 喷墨打印的 rGO/PVA 电极。**(b)** 石墨、氧化石墨、GO/PVA 和 rGO/PVA 复合材料的 XRD 图。插页显示了分散良好的 GO/PVA（左）和 rGO/PVA（右）悬浮液的照片。**(c)** 在含有 DMF 和水的混合溶剂中稳定分散三个月的 rGO/PVA 复

合材料（左）和从相同介质中析出的 rGO（右）。**(d)** 装置结构示意图。(插图：喷墨打印 rGO-PVA 复合电极的光学显微镜图像，比例尺：300 μm）。**(e)** 通过喷墨打印制作的 5 层和 20 层 rGO/PVA 薄膜照片。**(f)** 通过喷墨打印制作的 5 层和 20 层 rGO/PVA 薄膜的紫外-可见光谱。透射率在 λ = 550 nm 处测量。**(g)** 基于不同电极的有机场效应晶体管的输出特性：Au（左）、rGO/PVA（中）和 PEDOT:PSS（右）[57]。**(h)** 定向组装机制示意图。**(i)** 直方图显示了不含添加剂的 GO 悬浮液（1.75 wt%）（左）、低浓度氧化石墨烯的 GO/支链共聚物表面活性剂（branched copolymer surfactant, BCS）悬浮液（1.75 wt%，LC，中）和高浓度 GO/BCS 墨水（2.5 wt% GO，HC，右）的粘度和存储模量（G'）的比较。剪切速率为 10 s^{-1} 时的粘度从 10 Pa s 增加到近 50 Pa s。**(j)** 在固定应变（1%）和频率（0.1 Hz）下进行时间扫描后的自组装动力学[58]。

Figure 6. (a) Inkjet-printed rGO/PVA electrodes. **(b)** XRD patterns of graphite, graphite oxide (GO), GO/PVA, and rGO/PVA composite. The insert shows photographs of well-dispersed GO/PVA (left) and rGO/PVA (right) suspensions. **(c)** rGO/PVA composite stably dispersed in a mixed solvent with DMF and water for three months (left) and rGO precipitated from the same medium (right). **(d)** Schematic illustration of the device structure. (Insert: optical microscope image of inkjet-printed rGO-PVA composite electrodes, scale bar: 300 μm). **(e)** Photographs of rGO/PVA films with 5 and 20 layers fabricated by inkjet printing. **(f)** UV-vis spectra of rGO/PVA films with 5 and 20 layers fabricated by inkjet printing. Transmittance was measured at λ = 550 nm. **(g)** Output characteristics of organic field-effect transistors based on different electrodes: Au (left), rGO/PVA (center), and PEDOT:PSS (right)[57]. **(h)** Sketch of the directed assembly mechanism. **(i)** Histogram showing a comparison of the viscosity and storage modulus (G') of a GO suspension (1.75 wt%) without additives (left), a GO/branched copolymer surfactant (BCS) suspension with low graphene oxide concentration (1.75 wt%, LC, middle), and a highly concentrated GO/BCS ink (2.5 wt% GO, HC, right). The viscosity at a shear rate of 10 s^{-1} increases from 10 to nearly 50 Pa s. **(j)** Kinetics of self-assembly followed by a time sweep at a fixed strain (1%) and frequency (0.1 Hz)[58].

3.3. 立体光刻设备

立体光刻设备（stereo lithography apparatus, SLA）是一种使用感光树脂作为印刷材料的成型方法。具体来说，激光束按照设计的路线扫描液态感光树脂的表面，使感光树脂的特定区域固化，从而形成模型的横截面。随后，升降台向下移动一小段距离以固化新的截面层，直至形成完整的零件。光敏树脂一般包括聚合物单体或预聚物、光引发剂等成分[59]。较常用的光敏树脂类型包括不饱和聚酯、环氧丙烯酸酯、聚氨酯丙烯酸酯等。当使用立体光刻设备形成碳纳米材料/聚合物基复合材料时，通常将碳纳米材料溶解在溶剂中，然后添加到光敏树脂中。树脂或直接添加到树脂中混合，然后进行光固化[60]。

近年来，Zhou 等[61]将 GO 加入到聚乙二醇二丙烯酸酯（polyethylene glycol diacrylate, PEGDA）和甲基丙烯酸明胶（methacrylated gelatin, GelMA）的磷酸盐缓冲盐溶液（phosphate buffered saline, PBS）中，然后加入光引发剂形成光敏树脂，如**图 7** 所示。其中，GelMA 和 PEGDA 是两种常用的光固化生物材料。值得注意的是，GO 的加入可以促进生物干细胞的粘附和生长，诱导干细胞分化。研究结果表明，光敏树脂可用于光固化制备生物支架，促进人骨髓间充质干细胞分化形成软骨组织。此外，还有一些报道称，在用于印刷的商用光敏树脂中直接添加碳纳米材料，以改善其机械性能。还可以通过高温后处理去除聚合物，然后对 GO 进行热还原，制备出三维 rGO 结构。立体光刻设备因其打印精度高、表面质量好、可形成复杂结构等优点，已成为当前三维打印市场的主流技术之一。然而，该技术目前的瓶颈主要在于成本高以及残留光引发剂和未固化光敏树脂的毒性。此外，还必须防止碳纳米材料在印刷过程中从感光树脂中沉淀出来，从而导致碳纳米材料在复合材料中的分布不均匀。

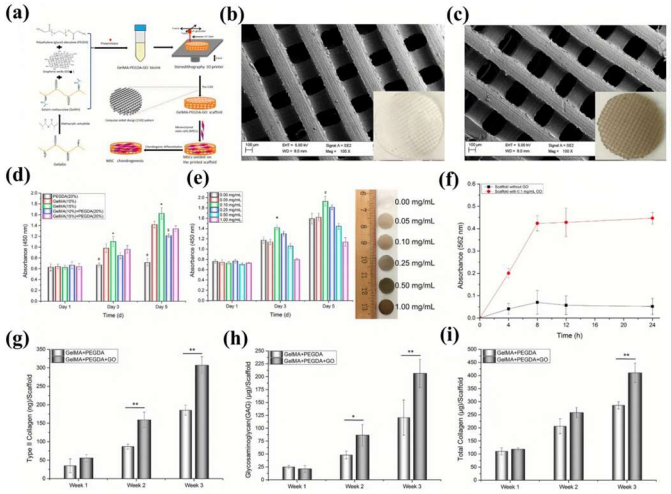

图 7. (a) 用于促进人骨髓间充质干细胞（human bone marrow mesenchymal stem cells, hMSC）软骨形成分化的 3D 打印 GO 支架示意图。**(b)**和**(c)**不含 GO 和含 GO（0.1 mg/mL）的 GelMA-PEGDA 支架的 SEM 显微照片。**(d)** 间充质干细胞（mesenchymal stem cell, MSC）在不同成分的水凝胶上增殖 5 天。**(e)** MSC 在掺有不同浓度 GO 的 GelMA-PEGDA 支架上增殖 5 天。**(f)** 不同时间点牛血清白蛋白（bovine serum albumin, BSA）在不含和含 GO（0.1 mg/mL）的 GelMA-PEGDA 支架上的吸附曲线。**(g)** 胶原蛋白 II。**(h)** 糖胺聚糖（glycosaminoglycan, GAG）和**(i)** 在含和含 GO 的 GelMA-PEGDA 支架上软骨分化后 3 周内 MSC 的总胶原蛋白分泌[61]。

Figure 7. (a) Schematic diagram of a 3D-printed GO scaffold for promoting chondrogenic differentiation of human bone marrow mesenchymal stem cells (hMSCs). **(b)** and **(c)** SEM micrographs of GelMA-PEGDA scaffolds without GO and with GO (0.1 mg/mL). **(d)** Mesenchymal stem cell (MSC) proliferation on hydrogels with different compositions for 5 d. **(e)** MSC proliferation on GelMA-PEGDA scaffolds incorporated with different concentrations of GO for 5 d. **(f)** Adsorption profiles of bovine serum albumin (BSA) on GelMA-PEGDA scaffolds with and without GO (0.1 mg/mL) at different time points. **(g)** Collagen II. (h) Glycosaminoglycan (GAG) and **(i)** total collagen secretion of MSCs after chondrogenic differentiation on GelMA-PEGDA scaffolds without and with GO over 3 weeks[61].

3.4. 选择性激光烧结技术

选择性激光烧结（selective laser sintering, SLS）是一种适用于粉末成型的3D打印方法，主要用于打印金属和陶瓷粉末，也可用于打印热塑性聚合物粉末[62]。在打印过程中，料筒首先上升一定距离，然后铺粉辊移动，在工作平台上铺上一层粉末材料[63,64]。然后，激光器发射激光束，所选区域的粉末在计算机控制下根据截面轮廓进行熔融烧结，从而增加层数。Gaikwad等[65]首先用双螺杆挤压机将碳纳米材料和尼龙11（PA11）熔化混合造粒，然后在低温下粉碎成粉末，用于选择性激光烧结，如**图8(c–e)**所示。研究结果表明，添加碳纳米材料不仅能提高尼龙11的弯曲模量、杨氏模量和热稳定性，还能使尼龙11具有导电性，可用于静电消散。与其他成型方法相比，通过选择性激光烧结获得的复合材料具有更好的导电性，而且静电消散所需的碳纳米材料用量较少。此外，碳纳米材料还能增强导热性，使激光熔化和烧结过程更加容易。

此外，Shuai等[66]首先用溶液混合法合成了GO/PVA复合粉末，然后用选择性激光烧结法制备了生物支架，如**图8(a,b,f–h)**所示。由于GO和PVA之间存在较强的氢键作用，二者结合紧密。研究结果表明，与纯树脂相比，添加了2.5% GO/PVA的支架的抗压强度、杨氏模量和拉伸强度分别提高了60%、152%和69%。选择性激光烧结的优点是可成型材料范围广，不同类型的粉末材料可以混合烧结形成复合材料，不需要支撑结构，材料利用率高。目前，关于选择性激光烧结形成碳纳米材料/聚合物基复合材料的报道较少。所报道的研究工作主要集中在尼龙基材料上，未来的研究可以扩展到更多类型的复合材料上。

近年来，研究人员在通过3D打印制备碳基聚合物复合材料方面取得了重大进展。然而，仍有一些问题亟待解决。一方面，在三维打印过程中容易出现喷嘴堵塞、结合力不足等问题，极大地影响

了碳基聚合物复合材料的性能。另一方面，目前可用于三维打印的聚合物种类相对有限，需要进一步拓展。

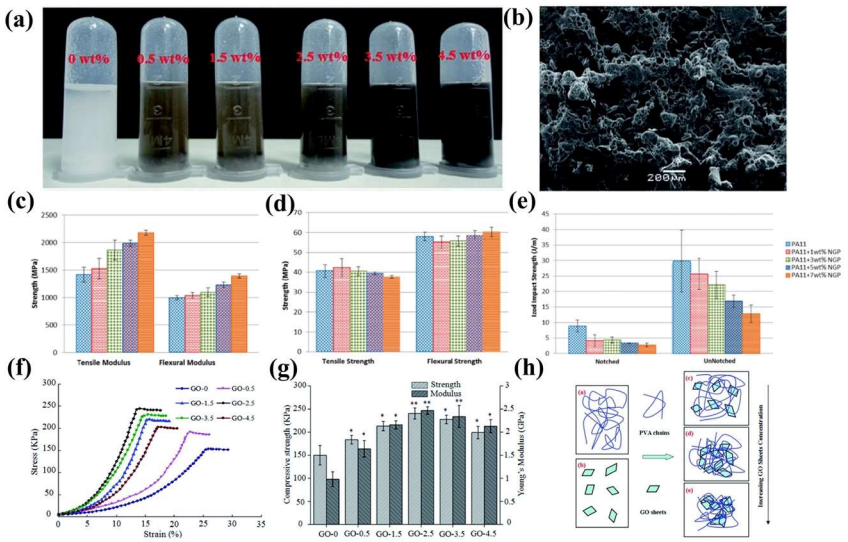

图8. (a) 超声分散后不同GO负载量的GO/PVA悬浮液的照片。**(b)** GO负载量为2.5 wt%的不同支架的表面形貌。**(c)** 拉伸强度和弯曲强度；**(d)** PA11和PA11/纳米石墨烯片（nanographene platelet, NGP）纳米复合材料的拉伸模量和弯曲模量。**(e)** 悬臂梁冲击强度[65]。**(f)** GO-0、GO-0.5、GO-1.5、GO-2.5、GO-3.5和GO-4.5应力-应变曲线的压缩特性。**(g)** GO-0、GO-0.5、GO-1.5、GO-2.5、GO-3.5和GO-4.5压缩强度和杨氏模量的压缩特性。**(h)** PVA链的示意图。**(a)** GO片材，以及**(b)** 不同GO负载量**(c)** 0.5 wt%、**(d)** 2.5 wt%和**(e)** 4.5 wt%的PVA基质中的GO片材分散体[66]。

Figure 8. (a) Photographs of GO/PVA suspension with different GO loadings after ultrasonic dispersion. **(b)** Surface morphologies of the scaffolds with different GO loadings of 2.5 wt%. **(c)** Tensile strength and flexural strength; and **(d)** Tensile modulus and flexure modulus of PA11 and PA11/ nanographene platelet (NGP) nanocomposites. **(e)** Izod impact strengths[65]. **(f)** Compressive properties of GO-0, GO-0.5, GO-1.5, GO-2.5, GO-3.5, and GO-4.5 stress-strain curves. **(g)** Compressive properties of GO-0, GO-0.5, GO-1.5, GO-2.5, GO-3.5, and GO-4.5 compressive strengths, and Young's modulus. **(h)** Schematic representation of the PVA chains. **(a)**, the GO sheets **(b)**, and the GO sheet dispersion in the PVA matrix with various GO loadings **(c)** 0.5 wt%, **(d)** 2.5 wt%, and **(e)** 4.5 wt%[66].

4. 碳基聚合物复合材料的应用

4.1. 电子领域

众所周知，碳纳米材料具有较大的比表面积和较高的载流子迁移率，这使得其在电子领域具有巨大的应用潜力[67–71]。碳纳米材料与合适的聚合物基体复合后可用于制备柔性电子器件[72,73]。3D 打印的应用可以方便、快速地形成复杂、精致的电子器件，并可以快速集成电子元件[74,75]。值得注意的是，石墨烯在电子领域研究的热点之一是石墨烯在场效应晶体管（field-effect transistors, FETs）中的应用。石墨烯较高的载流子迁移率使得石墨烯制成的晶体管具有更快的响应速度，可以显着提高晶体管的截止频率。另外，由于石墨烯厚度较小，可以减小晶体管的特征尺寸，摩尔定律可以进一步延续[76]，是未来集成电路领域的一个重要研究方向。

用于制备石墨烯 FETs 的 3D 打印方法主要是喷墨打印。最近，Xiang 等[77]通过喷墨印刷将石墨烯沉积在 Kapton 柔性基板上，并使用离子液体/共聚物凝胶作为栅极介电层来制备 FETs，如**图 9(a–c)**所示。发光二极管是一种光电器件，在通信、显示、照明等领域发挥着重要作用。石墨烯具有良好的透明和导电性能，可用作发光二极管的电极材料。研究人员制备了水凝胶状态的石墨烯用于喷墨打印[78]。此外，通过喷墨打印和熔融沉积建模等 3D 打印方法制备的电子电路可用于连接各种电子设备，如**图 9(d–h)**所示。

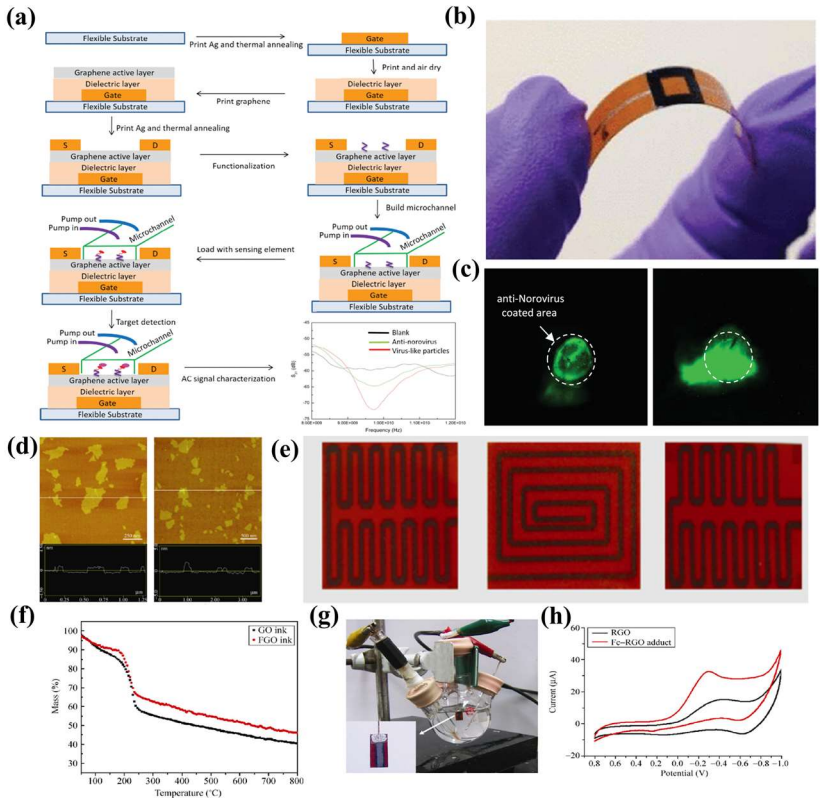

图9. (a) 石墨烯FET生物传感器的一般制造程序和信号输出。**(b)** 石墨烯FET生物传感器。**(c)** 使用荧光标记的二抗进行落射荧光染色，识别成功涂有目标特异性诺如病毒捕获抗体的印刷石墨烯区域。白色虚线圆圈表示一抗沉积的大致区域[77]。**(d)** GO墨水（0.1 mg/mL）中的GO片材和FGO墨水（0.1 mg/mL）中的少层氧化石墨烯（FGO）片材的典型敲击模式AFM图像（顶部）和相应的高度横截面轮廓（底部）沉积在云母基底上。**(e)** 使用浓度为5 mg/mL的FGO墨水在聚酰亚胺上打印图案。**(f)** GO墨水和FGO墨水中使用的氧化石墨烯材料在N_2气氛中在10 ℃升温速率下的TGA曲线。**(g)** H_2O_2传感器的CV测量。三电极法检测0.05 mol/L磷酸盐缓冲溶液（PBS）（ pH 7.4）和0.1 mol/L KCl中的H_2O_2。插图中显示的是裸露的印刷石墨烯电极。**(h)** rGO（黑色）和Fc-rGO加合物（Fc和还原氧化石墨烯杂化加合物）（红色）修饰印刷石墨烯电极在5 mmol/L H_2O_2、0.05 mol/L PBS（pH 7.4）中的循环伏安图，以及0.1 mol/L KCl被Ar饱和，扫描速率为50 mV/s[78]。

Figure 9. (a) General fabrication procedures and signal output of graphene FET biosensor. **(b)** Graphene FET biosensor. **(c)** Epifluorescence staining with a fluorescently-tagged secondary antibody identifies areas of printed graphene successfully coated with a target-specific Norovirus capture antibody. Dotted white circles indicate the approximate area of primary antibody deposition[77]. **(d)** Typical tapping mode AFM images (top) and the corresponding height cross-sectional profiles (bottom) of GO sheets in GO ink (0.1 mg/mL) and few-layered graphene oxide (FGO) sheets in FGO ink (0.1 mg/mL) deposited on mica substrate. **(e)** patterns printed on polyimide using FGO ink with a concentration of 5 mg/mL. **(f)** TGA curves of graphene oxide materials used in GO ink and FGO ink at a heating rate of 10 ℃ in an N_2 atmosphere. **(g)** CV measurements of the H_2O_2 sensors. The three-electrode method to detect H_2O_2 in 0.05 mol/L phosphate buffer solution (PBS) (pH 7.4) and 0.1 mol/L KCl. Shown in the inset is a bare-printed graphene electrode. **(h)** Cyclic voltammograms of rGO (black) and Fc-rGO adducts (the Fc and reduced graphene oxide hybrid adducts) (red) modified printed graphene electrodes in 5 mmol/L H_2O_2, 0.05 mol/L PBS (pH 7.4), and 0.1 mol/L KCl saturated with Ar at a 50 mV/s scan rate[78].

4.2. 航空航天领域

在航空航天领域，碳基聚合物复合材料也显示出相当大的应用潜力[79]。由于碳纳米材料具有优异的机械性能，将其添加到聚合物基体中可显著提高拉伸强度和弹性模量等机械性能[80–82]。众所周知，双马来酰亚胺、环氧树脂和酚醛树脂是航空航天领域常用的树脂基材[83]。值得注意的是，在这些树脂中加入少量碳纳米管、氧化石墨烯或改性石墨烯后，其机械性能会得到显著改善。除了用于改善机械性能，碳纳米材料还可用作功能增强材料。碳纳米材料可在聚合物基体中形成导电网络，提高复合材料的导电性，还可用于飞机的静电消散材料和雷击防护[84]。如**图 10(a–c)**所示，在聚合物基体中添加碳纳米材料还能增强复合材料的热稳定性，提高碳残留率，并可用于耐热材料的烧蚀。此外，碳基聚合物复合材料还可用于微波吸收和电磁屏蔽，并应用于飞机隐形领域[85]。由于碳纳米

材料在机械性能和功能性方面的优异表现，碳基聚合物复合材料还可用作未来飞机的结构/功能集成材料，如**图 10(d–g)**所示。三维打印技术可快速、精确地成型复杂部件的特点，与碳基聚合物复合材料优异的功能特性相结合，将在飞机非承重部件方面具有巨大的应用潜力。

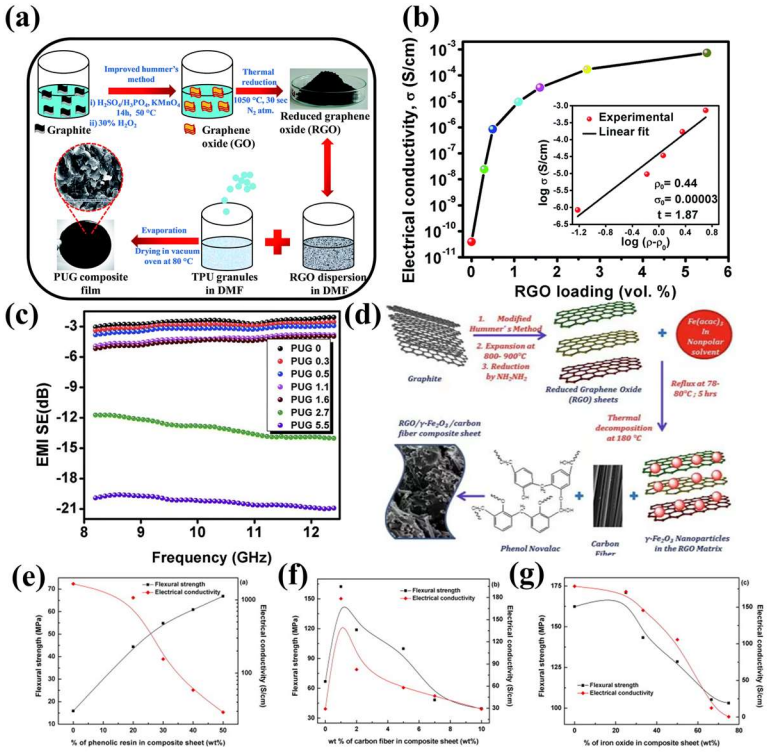

图10. (a) 聚氨酯石墨烯纳米复合薄膜的制造过程示意图。**(b)** 导电性随热塑性聚氨酯（thermoplastic polyurethanes, TPU）基体中rGO含量的变化。插图显示了log(σ) vs. log(ρ − ρ0)的对比图。**(c)** 聚氨酯/石墨烯（polyurethane/graphene, PUG）纳米复合材料的电磁干扰屏蔽效果随频率的变化[84]。**(d)** 有机介质中含有不同重量百分比rGO、γ-Fe_2O_3纳米粒子和碳纤维的酚醛树脂基复合材料片材的制备示意图。弯曲强度和导电率随rGO片材中**(e)** 酚醛树脂、**(f)** 碳纤维和**(g)** γ-Fe_2O_3的重量百分比的变化[85]。

Figure 10. (a) Schematic representation of the fabrication process of polyurethane graphene nanocomposite films. **(b)** Variation in electrical conductivity with rGO loading in the thermoplastic polyurethanes (TPU) matrix. The inset shows the log(σ) vs. log(ρ − ρ0) plot. **(c)** Variation in the EMI shielding effectiveness with frequency for polyurethane/graphene (PUG) nanocomposites[84]. **(d)** Schematic representation of the preparation of phenolic resin-based composite sheets containing different wt% of rGO, γ-Fe_2O_3 nanoparticles and carbon fibers in the organic medium. Variation of flexural strength and electrical conductivity as a function of wt% of **(e)** phenol resin, **(f)** carbon fiber, and **(g)** γ-Fe_2O_3 in rGO sheets[85].

4.3. 能源储存领域

基于碳纳米材料优异的导电性和低热膨胀系数，研究人员将碳纳米材料与正负极活性材料混合形成 3D 锂离子电池，或使用热响应油墨将碳纳米材料与铜粉混合形成超级电容器。深入研究了添加碳纳米材料的复合材料的高导电性和低电阻特性在锂离子电池和超级电容器中的潜在应用。最近，Fu 等[86]将水基墨水注入注射器，挤出细丝逐层打印，制备出电极，如**图 11(b–g)**所示。然后，将凝固的电极冷冻干燥并热退火，得到 rGO。磷酸铁锂（lithium iron phosphate, LFP）/rGO 和氧化钛锂（lithium titanium oxide, LTO）/rGO 电极分别采用上述 3D 打印方法制备。通过对其电化学性能的研究发现，加入 rGO 后，在比电流密度为 10 mA/g 时，两种锂离子电池几乎达到了磷酸铁锂和 LTO 的理论容量。其中，LTO/rGO 的初始充放电容量略高于 LTO 的理论容量。经过第 10 次和第 20 次循环后，两种电极的充放电曲线接近稳定，LTO/rGO 保持较低的电压滞后。

Rocha 等[87]以化学修饰石墨烯、与铜粉混合的水基热反应配方和 Pluronic F127（热反应油墨）为反应原料，通过 3D 打印和热处理方法制备了具有互锁界面的 rGO/Cu 电极，如**图 11(h–j)**所示。结果表明，电极产生的奈奎斯特图形状与理想超级电容器相同，表明 rGO 电极与铜电极之间接触良好。此外，Shen 等[88]将升华硫和 GO 溶液混合浓缩制备油墨，并通过挤出 3D 打印形成了具有周期性微晶格的硫共聚物-石墨烯结构（3DP-pSG），如**图 11(a)**所示。研究发现，该结构具有 812.8 mA h g^{-1} 的高可逆容量和良好的循环性能。最近，研究人员发现[89,90]，当聚合物复合材料中的碳纳米材料含量较高时，碳纳米材料可以形成更紧凑的微结构和连接良好的导电网络，电阻更低。上述研究工作为 3D 打印碳基聚合物复合材料在储能领域的应用提供了一些指导。

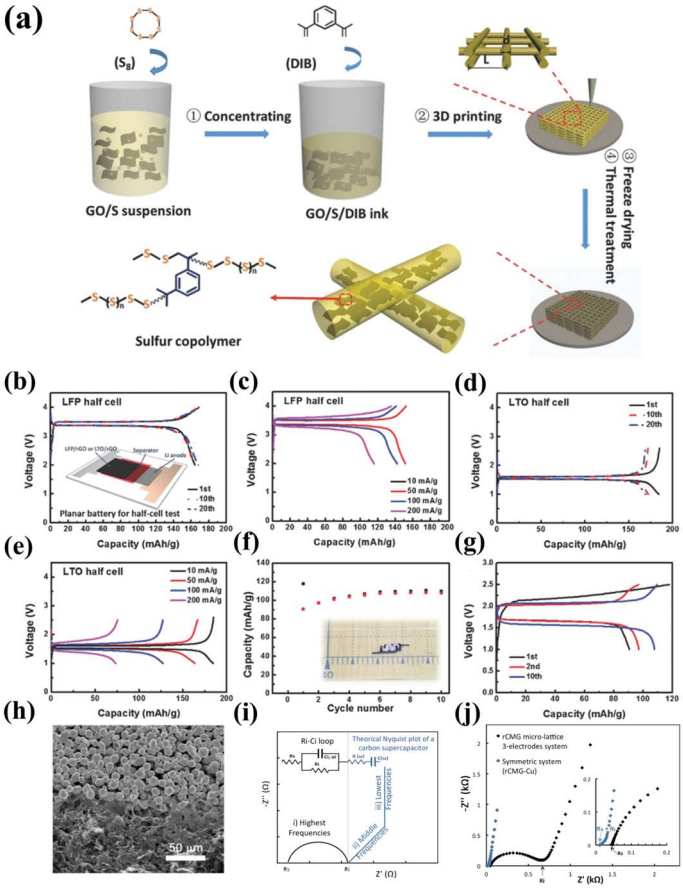

图 11. (a) 硫磺共聚物-石墨烯（3DP-pSG）架构的3D打印示意图。将水性GO悬浮液与升华硫均匀混合，浓缩成凝胶状油墨；然后将1,3-二异丙苯（diisopropenylbenzene, DIB）添加到油墨中并均匀混合。将制备好的油墨放入3 mL注射器中，逐层印刷成结构。然后，将印刷好的结构进行冷冻干燥。最后，通过200 ℃热处理在石墨烯纳米壁上合成硫共聚物[88]。**(b)** LFP/rGO半电池在10 mA g^{-1}特定电流下的充放电曲线。**(c)** LFP/rGO半电池在不同特定电流下的速率曲线。**(d)** LTO/rGO半电池在10 mA g^{-1}特定电流下的充放电曲线。**(e)** LTO/rGO半电池在不同特定电流下的速率曲线。**(f)** 3D打印全电池的循环稳定性。插图是由LFP/rGO、LTO/rGO和聚合物电解质组成的3D打印全电池的数字图像。**(g)** 3D打印全电池的充放电曲线[86]。**(h)** 还原化学修饰石墨烯（reduced chemically modified graphene, rCMG）/铜界面的SEM图像。**(i)** 碳-碳超级电容器的典型奈奎斯特图。它包括超级电容器从高频到低频的等效电路行为（Rs是高频电阻，Ri是活性材料/集流器界面的电阻，Ci是界面电容与分散参数αi、R(ω)是超级电容器电阻的一部分，取决于频率；C(ω)是超级电容器单元电容）和**(j)** 在EMI-TFSI电解液中记录的三电极系统（蓝色）和对称系统（黑色）从100 kHz到10 mHz的奈奎斯特图，以及相应的高频和中频响应放大图[87]。

Figure 11. (a) Schematic demonstration of 3D printing sulfur copolymer-graphene (3DP-pSG) architectures. Aqueous GO suspension was homogeneously mixed with sublimed sulfur and concentrated into gel-like ink; then, 1,3-diisopropenylbenzene (DIB) was added to the ink and mixed homogeneously. As-prepared ink was placed into a 3 mL syringe and printed into layer-by-layer architectures. Afterward, the printed architectures were freeze-dried. Finally, sulfur copolymer was synthesized on the graphene nanowalls by thermal treatment at 200 ℃[88]. **(b)** Charge and discharge profiles of the LFP/rGO half-cell at a specific current of 10 mA g^{-1}. **(c)** Rate profiles of the LFP/rGO half-cell at various specific currents. **(d)** Charge and discharge profiles of the LTO/rGO

half-cell at a specific current of 10 mA g^{-1}. **(e)** Rate profiles of the LTO/rGO half-cell at various specific currents. **(f)** Cycling stability of the 3D-printed full cell. The inset is a digital image of the 3D-printed full cell consisting of LFP/rGO, LTO/rGO, and polymer electrolyte. **(g)** Charge and discharge profiles of the 3D-printed full cell[86]. **(h)** SEM images at the reduced chemically modified graphene(rCMG)/Cu interface. **(i)** Typical Nyquist plot of a carbon–carbon supercapacitor. It includes the high- to low-frequency behavior of a supercapacitor with the equivalent circuits (Rs is the high-frequency resistance, Ri is the resistance of the active material/current collector interface, Ci is the interface capacitance with the dispersion parameter αi, R(ω) is a part of the supercapacitor resistance depending on the frequency, and C(ω) is the supercapacitor cell capacitance) and **(j)** Nyquist plots recorded from 100 kHz to 10 mHz for the three-electrode (blue) and symmetric (black) systems in EMI-TFSI electrolyte, with their corresponding magnification of high and mid-frequency response[87].

4.4. 生物医学领域

许多研究人员利用三维打印技术将生物相容性高分子材料和碳纳米材料制成水凝胶、三维支架和导管[91–93]。然后，通过体外实验模拟其对骨组织、神经组织和细胞增殖的影响，发现低含量的碳纳米材料对生物细胞无毒[94–96]。同样，碳纳米材料具有良好的生物相容性，不仅能增强生物材料的硬度，还能促进细胞增殖[97,98]。这为组织工程和生物医学研究提供了广阔的前景[99]。

用于制造水凝胶结构的 3D 打印技术的发展使得大规模生产工程软骨组织成为可能。最近，Wang 等[100]使用 NaOH 溶液处理含有低浓度石墨烯的 3D 打印聚（ε-己内酯）（PCL）支架，如**图 12(b)**所示。研究结果表明，经 NaOH 处理的支架与细胞的生物相容性更好。Cheng 等[101]将 3D 生物打印显微注射系统与生物聚合物储库连接起来，使用软骨细胞接种 GO/壳聚糖水凝胶，如**图 12(c,d)**所示。研究结果表明，与纯水凝胶相比，3D 打印的 GO/水凝胶组织移植到软骨组织后具有更厚的新生软骨。此外，Chen 等[102]将 TPU 和 GO 分别溶解在二甲基甲酰胺（dimethylformamide, DMF）中，将 PLA 溶解在二氯甲烷（dichloromethane, DCM）中，如**图 12(a,g–j)**所示。然后，使用挤出机将混合物沉淀并干燥，制成复合长丝，可直接在 FDM 打印机中使用。研究结果表明，添加 GO 的复合材料的力学性能和热稳定性显着提高，且支架与 NIH_3T_3 细胞表现出良好的生物相容性。Sayyar 等[103]采用挤出沉积 3D 打印方法成功制备了聚三亚甲基碳酸酯（polytrimethylene carbonate, PTMC）/碳纳米材料复合材料，如**图 12(e,f)**所示。通过添加碳纳米材料前后的对比实验发现，两种支架上细胞的 DNA 含量没有显着差异。这表明碳纳米材料的添加对细胞数量没有影响。因此，碳基聚合物复合材料在生物医用材料领域，特别是在组织工程新型导电支架的开发方面具有重要的应用前景。

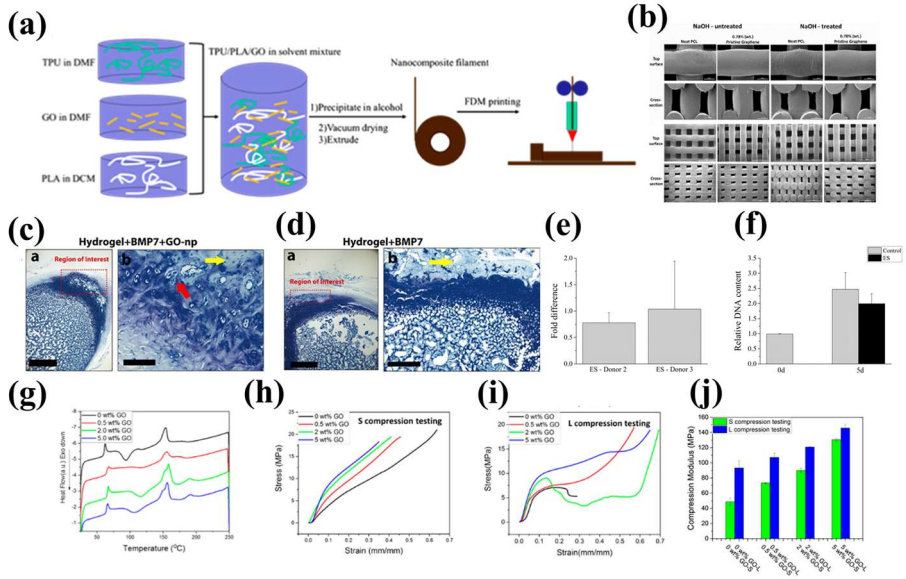

图 12. (a) TPU/PLA/GO纳米复合材料长丝制备和FDM印刷过程[102]。**(b)** 经NaOH处理和未处理的纯PCL和0.78 wt%原始石墨烯支架的顶面和横截面扫描电子显微镜图像[100]。**(c)** 水凝胶 + BMP7 + GO-np移植到大鼠膝关节软骨中的甲苯胺染色图。**(d)**

水凝胶 + BMP7 + 移植到大鼠膝关节软骨中的甲苯胺染色图。在相关区域，水凝胶 + BMP7 组的新生软骨比水凝胶 + BMP7 + GO-np （氧化石墨烯纳米颗粒）组更薄（黄色箭头），水凝胶 + BMP7 组未观察到新生软骨细胞（红色箭头）[101]。**(e)** 相对于未受刺激的对照组，电刺激（electrical stimulation, ES）对间充质干细胞（mesenchymal stem cell, MSC）数量的影响。结果显示为ES 5天后相对于未刺激对照组的倍数差异。**(f)** 在两个时间点测量的细胞数量（供体2）[103]。**(g)** 不同GO含量下样品的差示扫描量热曲线。**(h)** 不同负载量GO样品的S压缩测试曲线。**(i)** 不同GO负载下样品的L压缩测试曲线。**(j)** 不同负载量的GO样品的L和S压缩测试压缩模量[102]。

Figure 12. (a) TPU/PLA/GO nanocomposites filament preparation and FDM printing process[102]. **(b)** Top surface and cross-section scanning electron microscope images of neat PCL and 0.78 wt% pristine graphene scaffolds treated and untreated with NaOH[100]. **(c)** Toluidine staining of hydrogel + BMP7 + GO-np transplanted in cartilage of rat knees. **(d)** Toluidine staining of hydrogel + BMP7 + transplanted in cartilage of rat knees. In the region of interest, the neogenetic cartilage of the hydrogel + BMP7 was thinner than hydrogel + BMP7 + GO-np (graphene oxide nanoparticels) (yellow arrow), and no neogenetic chondrocytes were observed in the hydrogel + BMP7 group (red arrow)[101]. **(e)** Effect of electrical stimulation (ES) on mesenchymal stem cell (MSC) numbers relative to unstimulated controls. Results are shown as a fold difference relative to the unstimulated control after five days of ES. **(f)** Cell number measured at two time points (donor 2)[103]. **(g)** Differential scanning calorimetry (DSC) curves of samples at different GO loadings. **(h)** S compression testing curves of samples of different GO loadings. **(i)** L compression testing curves of samples of different GO loadings. **(j)** Compression modulus of L and S compression testing of samples of different GO loadings[102].

5. 总结与展望

碳基聚合物基复合材料和三维打印是近年来发展迅速的两个研究方向。将两者结合起来，发挥各自的优势，可以为碳基聚合物复合材料的复杂结构成型提供有效的解决方案。因此，利用碳基填料制备的可拉伸导电纳米复合材料为下一代电子设备提供了一个新的研究方向。然而，基于纳米碳填料的可拉伸导电聚合物复合材料的研究和应用仍处于起步阶段，还面临着许多问题和挑战。主要包括以下三个方面：(i) 在现有的复合方法中，碳纳米材料在聚合物载体中的分散性较差，导致无法充分发挥碳纳米材料优异的力学和电学性能；(ii) 3D 打印过程中容易出现喷嘴堵塞、结合力不足等问题，极大地影响了碳基聚合物复合材料的性能；(iii) 目前可用于 3D 打印的聚合物种类相对有限，需要进一步拓展。

基于纳米碳填料的可拉伸导电聚合物复合材料的未来研究将主要集中在以下几个方面：(i) 选择合适的混合方法并使用某些化学添加剂来改善导电填料在聚合物中的分散性。(ii) 多种碳纳米材料配合使用，构建稳定高效的导电网络。(iii) 碳纳米材料具有很强的改性能力，可根据具体应用进行改性。(iv) 通过开发新型印刷技术，可实现可拉伸电子器件的微型化和大规模制造。通过对现有研究的总结，相信基于纳米碳填料制备的可拉伸导电聚合物复合材料可以应用于可拉伸电子器件等多个领域，促进相关研究领域的进步。

致谢

本研究得到了上海市基础研究特区项目（批准号：22TQ1400100-8）、上海市浦江人才计划（批准号：20PJ1402500）、上海市自然科学基金（批准号：22ZR1416600）和中央高校基本科研业务费的资助。

利益冲突

作者声明无利益冲突。

参考文献

1. Cao D, Xing Y, Tantratian K, et al. 3D printed high-performance lithium metal microbatteries enabled by nanocellulose. *Advanced Materials* 2019; 31(14): 1807313. doi: 10.1002/adma.201807313
2. Chen X. Making electrodes stretchable. *Small Methods* 2017; 1(4): 1600029. doi: 10.1002/smtd.201600029
3. Lv Z, Li W, Yang L, et al. Custom-made electrochemical energy storage devices. *ACS Energy Letters* 2019; 4(2): 606–614. doi: 10.1021/acsenergylett.8b02408
4. Zhao C, Wang R, Fang B, et al. Boosting the lithium storage properties of a flexible $Li_4Ti_5O_{12}$/graphene fiber

anode via a 3D printing assembly strategy. *Batteries* 2023; 9(10): 493. doi: 10.3390/batteries9100493
5. Wang C, Xia K, Wang H, et al. Advanced carbon for flexible and wearable electronics. *Advanced Materials* 2019; 31(9): 1801072. doi: 10.1002/adma.201801072
6. Bokobza L. Mechanical and electrical properties of elastomer nanocomposites based on different carbon nanomaterials. *C—Journal of Carbon Research* 2017; 3(2): 10. doi: 10.3390/c3020010
7. Mondal S, Khastgir D. Elastomer reinforcement by graphene nanoplatelets and synergistic improvements of electrical and mechanical properties of composites by hybrid nano fillers of graphene-carbon black & graphene-MWCNT. *Composites Part A: Applied Science and Manufacturing* 2017; 102: 154–165. doi: 10.1016/j.compositesa.2017.08.003
8. Ryan KR, Down MP, Hurst NJ, et al. Additive manufacturing (3D printing) of electrically conductive polymers and polymer nanocomposites and their applications. *eScience* 2022; 2(4): 365–381. doi: 10.1016/j.esci.2022.07.003
9. Huang A, Ma Y, Peng J, et al. Tailoring the structure of silicon-based materials for lithium-ion batteries via electrospinning technology. *eScience* 2021; 1(2): 141–162. doi: 10.1016/j.esci.2021.11.006
10. Wang Z, Gao W, Zhang Q, et al. 3D-printed graphene/polydimethylsiloxane composites for stretchable and strain-insensitive temperature sensors. *ACS Applied Materials & Interfaces* 2019; 11(1): 1344–1352. doi: 10.1021/acsami.8b16139
11. Mo R, Rooney D, Sun K, Yang HY. 3D nitrogen-doped graphene foam with encapsulated germanium/nitrogen-doped graphene yolk-shell nanoarchitecture for high-performance flexible Li-ion battery. *Nature Communications* 2017; 8(1): 13949. doi: 10.1038/ncomms13949
12. Zhao C, Liang H, Wang R, et al. Recent advances in high value-added carbon materials prepared from carbon dioxide for energy storage applications. *Carbon Capture Science & Technology* 2023; 9: 100144. doi: 10.1016/j.ccst.2023.100144
13. de Leon AC, Chen Q, Palaganas NB, et al. High performance polymer nanocomposites for additive manufacturing applications. *Reactive and Functional Polymers* 2016; 103: 141–155. doi: 10.1016/j.reactfunctpolym.2016.04.010
14. Song WJ, Lee S, Song G, Park S. Stretchable aqueous batteries: Progress and prospects. *ACS Energy Letters* 2019; 4(1): 177–186. doi: 10.1021/acsenergylett.8b02053
15. Song Z, Ma T, Tang R, et al. Origami lithium-ion batteries. *Nature Communications* 2014; 5(1): 3140. doi: 10.1038/ncomms4140
16. Bao Y, Zhang XY, Zhang X, et al. Free-standing and flexible limntio_4/carbon nanotube cathodes for high performance lithium ion batteries. *Journal of Power Sources* 2016; 321: 120–125. doi: 10.1016/j.jpowsour.2016.04.121
17. Fu KK, Cheng J, Li T, Hu L. Flexible batteries: From mechanics to devices. *ACS Energy Letters* 2016; 1(5): 1065–1079. doi: 10.1021/acsenergylett.6b00401
18. Bao Y, Hong G, Chen Y, et al. Customized kirigami electrodes for flexible and deformable lithium-ion batteries. *ACS Applied Materials & Interfaces* 2020; 12(1): 780–788. doi: 10.1021/acsami.9b18232
19. Storck JL, Ehrmann G, Uthoff J, Diestelhorst E. Investigating inexpensive polymeric 3D printed materials under extreme thermal conditions. *Materials Futures* 2022; 1(1): 015001. doi: 10.1088/2752-5724/ac4beb
20. de Castro Motta J, Qaderi S, Farina I, et al. Experimental characterization and mechanical modeling of additively manufactured TPU components of innovative seismic isolators. *Acta Mechanica* 2022. doi: 10.1007/s00707-022-03447-5
21. Buchanan C, Gardner L. Metal 3D printing in construction: A review of methods, research, applications, opportunities and challenges. *Engineering Structures* 2019; 180: 332–348. doi: 10.1016/j.engstruct.2018.11.045
22. Zhu C, Liu T, Qian F, et al. 3D printed functional nanomaterials for electrochemical energy storage. *Nano Today* 2017; 15: 107–120. doi: 10.1016/j.nantod.2017.06.007
23. Zhang F, Wei M, Viswanathan VV, et al. 3D printing technologies for electrochemical energy storage. *Nano Energy* 2017; 40: 418–431. doi: 10.1016/j.nanoen.2017.08.037
24. Sousa RE, Costa CM, Lanceros-Méndez S. Advances and future challenges in printed batteries. *ChemSusChem* 2015; 8(21): 3539–3555. doi: 10.1002/cssc.201500657
25. Tian X, Jin J, Yuan S, et al. Emerging 3D-printed electrochemical energy storage devices: A critical review. *Advanced Energy Materials* 2017; 7(17): 1700127. doi: 10.1002/aenm.201700127
26. Guo W, Wang X, Yang C, et al. Microfluidic 3D printing polyhydroxyalkanoates-based bionic skin for wound healing. *Materials Futures* 2022; 1: 015401. doi: 10.1088/2752-5724/ac446b
27. Park S, Shou W, Makatura L, et al. 3D printing of polymer composites: Materials, processes, and applications. *Matter* 2022; 5(1): 43–76. doi: 10.1016/j.matt.2021.10.018
28. de Leon AC, Rodier BJ, Bajamundi C, et al. Plastic metal-free electric motor by 3D printing of graphene-polyamide powder. *ACS Applied Energy Materials* 2018; 1(4): 1726–1733. doi: 10.1021/acsaem.8b00240
29. Hall A, Kong GX, Karanassios V. Detectors and light-sources for optical spectrometry: From a 3D-printed light-source to a self-powered sensor fabricated on a flexible polymeric substrate, and from there on to an IoT-enabled

"smart" system. In: Proceedings of the 2019 IEEE International Conference on Flexible and Printable Sensors and Systems (FLEPS); 8–10 July 2019; Glasgow, UK. pp. 1–3. doi:10.1109/fleps.2019.8792321
30. Kurra N, Jiang Q, Nayak P, Alshareef HN. Laser-derived graphene: A three-dimensional printed graphene electrode and its emerging applications. *Nano Today* 2019; 24: 81–102. doi: 10.1016/j.nantod.2018.12.003
31. Li C, Cheng J, He Y, et al. Polyelectrolyte elastomer-based ionotronic sensors with multi-mode sensing capabilities via multi-material 3D printing. *Nature Communications* 2023; 14(1): 4853. doi: 10.1038/s41467-023-40583-5
32. Li K, Liang M, Wang H, et al. 3D mxene architectures for efficient energy storage and conversion. *Advanced Functional Materials* 2020; 30(47): 2000842. doi: 10.1002/adfm.202000842
33. Lyu Z, Lim GJH, Koh JJ, et al. Design and manufacture of 3D-printed batteries. *Joule* 2021; 5(1): 89–114. doi: 10.1016/j.joule.2020.11.010
34. Park J, Kim JK, Park SA, et al. 3D-printed biodegradable polymeric stent integrated with a battery-less pressure sensor for biomedical applications. In: Proceedings of the 2017 19th International Conference on Solid-State Sensors, Actuators and Microsystems (TRANSDUCERS); 18–22 June 2017; Kaohsiung, Taiwan. pp. 14–50. doi: 10.1109/transducers.2017.7993984
35. Ngo TD, Kashani A, Imbalzano G, et al. Additive manufacturing (3D printing): A review of materials, methods, applications and challenges. *Composites Part B: Engineering* 2018; 143: 172–196. doi: 10.1016/j.compositesb.2018.02.012
36. Zhu Y, Murali S, Cai W, et al. Graphene and graphene oxide: Synthesis, properties, and applications. *Advanced Materials* 2010; 22(35): 3906–3024. doi: 10.1002/adma.201001068
37. Unwin PR, Güell AG, Zhang G. Nanoscale electrochemistry of sp^2 carbon materials: From graphite and graphene to carbon nanotubes. *Accounts of Chemical Research* 2016; 49(9): 2041–2408. doi: 10.1021/acs.accounts.6b00301
38. Smith M. New developments in carbon fiber. *Reinforced Plastics* 2018; 62(5): 266–269. doi: 10.1016/j.repl.2017.07.004
39. Fu X, Xu L, Li J, et al. Flexible solar cells based on carbon nanomaterials. *Carbon* 2018; 139: 1063–1073. doi: 10.1016/j.carbon.2018.08.017
40. Bhagavatheswaran ES, Parsekar M, Das A, et al. Construction of an interconnected nanostructured carbon black network: Development of highly stretchable and robust elastomeric conductors. *The Journal of Physical Chemistry C* 2015; 119(37): 21723–21731. doi: 10.1021/acs.jpcc.5b06629
41. Niu XZ, Peng SL, Liu LY, et al. Characterizing and patterning of PDMS-based conducting composites. *Advanced Materials* 2007; 19(18): 2682–2686. doi: 10.1002/adma.200602515
42. Song WJ, Park J, Kim DH, et al. Jabuticaba-inspired hybrid carbon filler/polymer electrode for use in highly stretchable aqueous Li-ion batteries. *Advanced Energy Materials* 2018; 8(10): 1702478. doi: 10.1002/aenm.201702478
43. Shin MK, Oh J, Lima M, et al. Elastomeric conductive composites based on carbon nanotube forests. *Advanced Materials* 2010; 22(24): 2663–2667. doi: 10.1002/adma.200904270
44. Sekitani T, Nakajima H, Maeda H, et al. Stretchable active-matrix organic light-emitting diode display using printable elastic conductors. *Nature Materials* 2009; 8(6): 494–499. doi: 10.1038/nmat2459
45. Liu Z, Qian Z, Song J, Zhang Y. Conducting and stretchable composites using sandwiched graphene-carbon nanotube hybrids and styrene-butadiene rubber. *Carbon* 2019; 149: 181–189. doi: 10.1016/j.carbon.2019.04.037
46. Gao N, Fang X. Synthesis and development of graphene—Inorganic semiconductor nanocomposites. *Chemical Reviews* 2015; 115(16): 8294–83343. doi: 10.1021/cr400607y
47. Chen Z, Ren W, Gao L, et al. Three-dimensional flexible and conductive interconnected graphene networks grown by chemical vapour deposition. *Nature Materials* 2011; 10(6): 424–428. doi: 10.1038/nmat3001
48. Wang Z, Liu X, Shen X, et al. An ultralight graphene honeycomb sandwich for stretchable light-emitting displays. *Advanced Functional Materials* 2018; 28(19): 1707043. doi: 10.1002/adfm.201707043
49. Sun F, Tian M, Sun X, et al. Stretchable conductive fibers of ultrahigh tensile strain and stable conductance enabled by a worm-shaped graphene microlayer. *Nano Letters* 2019; 19(9): 6592–6599. doi: 10.1021/acs.nanolett.9b02862
50. Praveena BA, Lokesh N, Buradi A, et al. A comprehensive review of emerging additive manufacturing (3D printing technology): Methods, materials, applications, challenges, trends and future potential. *Materials Today: Proceedings* 2022; 52(Part 3): 1309–1313. doi: 10.1016/J.MATPR.2021.11.059
51. Kristiawan RB, Imaduddin F, Ariawan D, et al. A review on the fused deposition modeling (FDM) 3D printing: Filament processing, materials, and printing parameters. *Open Engineering* 2021; 11(1): 639–649. doi: 10.1515/ENG-2021-0063
52. Pervaiz S, Qureshi TA, Kashwani G, Kannan S. 3D printing of fiber-reinforced plastic composites using fused deposition modeling: A status review. *Materials* 2021; 14(16): 4520. doi: 10.3390/MA14164520
53. Wei X, Li D, Jiang W, et al. 3D printable graphene composite. *Scientific Reports* 2015; 5(1): 11181. doi: 10.1038/srep11181

54. Zhu D, Ren Y, Liao G, et al. Thermal and mechanical properties of polyamide 12/graphene nanoplatelets nanocomposites and parts fabricated by fused deposition modeling. *Journal of Applied Polymer Science* 2017; 134(39): 45332. doi: 10.1002/app.45332
55. Saadi MASR, Maguire A, Pottackal NT, et al. Direct ink writing: A 3D printing technology for diverse materials. *Advanced Materials* 2022; 34(28): 2108855. doi: 10.1002/ADMA.202108855
56. Singh M, Haverinen HM, Dhagat P, Jabbour GE. Inkjet printing—Process and its applications. *Advanced Materials* 2010; 22(6): 673–685. doi: 10.1002/adma.200901141
57. Lim S, Kang B, Kwak D, et al. Inkjet-printed reduced graphene oxide/poly(vinyl alcohol) composite electrodes for flexible transparent organic field-effect transistors. *The Journal of Physical Chemistry C* 2012; 116(13): 7520–7525. doi: 10.1021/jp203441e
58. García-Tuñon E, Barg S, Franco J, et al. Printing in three dimensions with graphene. *Advanced Materials* 2015; 27(10): 1688–1693. doi: 10.1002/adma.201405046
59. Uçak N, Çiçek A, Aslantas K. Machinability of 3D printed metallic materials fabricated by selective laser melting and electron beam melting: A review. *Journal of Manufacturing Processes* 2022; 80: 414–457. doi: 10.1016/J.JMAPRO.2022.06.023
60. Acord KA, Dupuy AD, Scipioni Bertoli U, et al. Morphology, microstructure, and phase states in selective laser sintered lithium ion battery cathodes. *Journal of Materials Processing Technology* 2021; 288: 116827. doi: 10.1016/J.JMATPROTEC.2020.116827
61. Zhou X, Nowicki M, Cui H, et al. 3D bioprinted graphene oxide-incorporated matrix for promoting chondrogenic differentiation of human bone marrow mesenchymal stem cells. *Carbon* 2017; 116: 615–624. doi: 10.1016/j.carbon.2017.02.049
62. Pagac M, Hajnys J, Ma QP, et al. A review of vat photopolymerization technology: Materials, applications, challenges, and future trends of 3D printing. *Polymers* 2021; 13(4): 598. doi: 10.3390/POLYM13040598
63. Costa BMDC, Griveau S, Bedioui F, et al. Stereolithography based 3D-printed microfluidic device with integrated electrochemical detection. *Electrochimica Acta* 2022; 407: 139888. doi: 10.1016/J.ELECTACTA.2022.139888
64. Li C, Du J, Gao Y, et al. Stereolithography of 3D sustainable metal electrodes towards high-performance nickel iron battery. *Advanced Functional Materials* 2022; 32(40): 2205317. doi: 10.1002/ADFM.202205317
65. Gaikwad S, Tate JS, Theodoropoulou N, Koo JH. Electrical and mechanical properties of PA11 blended with nanographene platelets using industrial twin-screw extruder for selective laser sintering. *Journal of Composite Materials* 2013; 47(23): 2973–2986. doi: 10.1177/0021998312460560
66. Shuai C, Feng P, Gao C, et al. Graphene oxide reinforced poly(vinyl alcohol): Nanocomposite scaffolds for tissue engineering applications. *RSC Advances* 2015; 5: 25416–25423. doi: 10.1039/C4RA16702C
67. Zhai F, Feng Y, Li Z, et al. 4D-printed untethered self-propelling soft robot with tactile perception: Rolling, racing, and exploring. *Matter* 2021; 4(10): 3313–3326. doi: 10.1016/J.MATT.2021.08.014
68. Yu Y, Feng Y, Liu F, et al. Carbon dots-based ultrastretchable and conductive hydrogels for high-performance tactile sensors and self-powered electronic skin. *Small* 2023; 19(31): 2204365. doi: 10.1002/SMLL.202204365
69. Zhu Y, Tang T, Zhao S, et al. Recent advancements and applications in 3D printing of functional optics. *Additive Manufacturing* 2022; 52: 102682. doi: 10.1016/J.ADDMA.2022.102682
70. Jiang Y, Islam MN, He R, et al. Recent advances in 3D printed sensors: Materials, design, and manufacturing. *Advanced Materials Technologies* 2023; 8(2): 2200492. doi: 10.1002/ADMT.202200492
71. Tan HW, Choong YYC, Kuo CN, et al. 3D printed electronics: Processes, materials and future trends. *Progress in Materials Science* 2022; 127: 100945. doi: 10.1016/J.PMATSCI.2022.100945
72. Zhang F, Feng Y, Feng W. Three-dimensional interconnected networks for thermally conductive polymer composites: Design, preparation, properties, and mechanisms. *Materials Science and Engineering: R: Reports* 2020; 142: 100580. doi: 10.1016/J.MSER.2020.100580
73. Li Z, Wang L, Li Y, et al. Carbon-based functional nanomaterials: Preparation, properties and applications. *Composites Science and Technology* 2019; 179: 10–40. doi: 10.1016/J.COMPSCITECH.2019.04.028
74. Zhang D, Chi B, Li B, et al. Fabrication of highly conductive graphene flexible circuits by 3D printing. *Synthetic Metals* 2016; 217: 79–86. doi: 10.1016/j.synthmet.2016.03.014
75. Liu H, Zhang H, Han W, et al. 3D printed flexible strain sensors: From printing to devices and signals. *Advanced Materials* 2021; 33(8): 2004782. doi: 10.1002/ADMA.202004782
76. Schwierz F. Graphene transistors. *Nature Nanotechnology* 2010;5(7): 487–496. doi: 10.1038/nnano.2010.89
77. Xiang L, Wang Z, Liu Z, et al. Inkjet-printed flexible biosensor based on graphene field effect transistor. *IEEE Sensors Journal* 2016; 16(23): 8359–8364. doi: 10.1109/JSEN.2016.2608719
78. Huang L, Huang Y, Liang J, et al. Graphene-based conducting inks for direct inkjet printing of flexible conductive patterns and their applications in electric circuits and chemical sensors. *Nano Research* 2011; 4(7): 675–684. doi: 10.1007/s12274-011-0123-z
79. Willian MD, Michaela E, Mae CH, et al. A comprehensive review on the application of 3D printing in the aerospace industry. *Key Engineering Materials* 2022; 913: 27–34. doi: 10.4028/p-94a9zb

80. Mohanavel V, Ashraff Ali KS, Ranganathan K, et al. The roles and applications of additive manufacturing in the aerospace and automobile sector. *Materials Today: Proceedings* 2021; 47: 405–409. doi: 10.1016/J.MATPR.2021.04.596
81. Sugiyama K, Matsuzaki R, Ueda M, et al. 3D printing of composite sandwich structures using continuous carbon fiber and fiber tension. *Composites Part A: Applied Science and Manufacturing* 2018; 113: 114–121. doi: 10.1016/J.COMPOSITESA.2018.07.029
82. Sai Saran O, Prudhvidhar Reddy A, Chaturya L, Pavan Kumar M. 3D printing of composite materials: A short review. *Materials Today: Proceedings* 2022; 64: 615–619. doi: 10.1016/J.MATPR.2022.05.144
83. Wang X, Jin J, Song M. An investigation of the mechanism of graphene toughening epoxy. *Carbon* 2013; 65: 324–333. doi: 10.1016/j.carbon.2013.08.032
84. Verma M, Verma P, Dhawan SK, Choudhary V. Tailored graphene based polyurethane composites for efficient electrostatic dissipation and electromagnetic interference shielding applications. *RSC Advances* 2015; 5(118): 97349–97358. doi: 10.1039/C5RA17276D
85. Singh AP, Garg P, Alam F, et al. Phenolic resin-based composite sheets filled with mixtures of reduced graphene oxide, γ-Fe_2O_3 and carbon fibers for excellent electromagnetic interference shielding in the X-band. *Carbon* 2012; 50(10): 3868–3875. doi: 10.1016/j.carbon.2012.04.030
86. Fu K, Wang Y, Yan C, et al. Graphene oxide-based electrode inks for 3D-printed lithium-ion batteries. *Advanced Materials* 2016; 28(13): 2587–2594. doi: 10.1002/adma.201505391
87. Rocha VG, García-Tuñón E, Botas C, et al. Multimaterial 3D printing of graphene-based electrodes for electrochemical energy storage using thermoresponsive inks. *ACS Applied Materials &Interfaces* 2017; 9(42): 37136–37145. doi: 10.1021/acsami.7b10285
88. Shen K, Mei H, Li B, et al. 3D printing sulfur copolymer-graphene architectures for Li-S batteries. *Advanced Energy Materials* 2018; 8(4): 1701527. doi: 10.1002/aenm.201701527
89. Huang K, Yang J, Dong S, et al. Anisotropy of graphene scaffolds assembled by three-dimensional printing. *Carbon* 2018; 130: 1–10. doi: 10.1016/j.carbon.2017.12.120
90. Vernardou D, Vasilopoulos KC, Kenanakis G. 3D printed graphene-based electrodes with high electrochemical performance. *Applied Physics A* 2017; 123: 623. doi: 10.1007/s00339-017-1238-1
91. Fan D, Li Y, Wang X, et al. Progressive 3D printing technology and its application in medical materials. *Frontiers in Pharmacology* 2020; 11: 516624. doi: 10.3389/FPHAR.2020.00122/BIBTEX
92. Al-Dulimi Z, Wallis M, Tan DK, et al. 3D printing technology as innovative solutions for biomedical applications. *Drug Discovery Today* 2021; 26(2): 360–383. doi: 10.1016/J.DRUDIS.2020.11.013
93. Chadha U, Abrol A, Vora NP, et al. Performance evaluation of 3D printing technologies: A review, recent advances, current challenges, and future directions. *Progress in Additive Manufacturing* 2022; 7(5): 853–886. doi: 10.1007/S40964-021-00257-4
94. Mallakpour S, Tabesh F, Hussain CM. 3D and 4D printing: From innovation to evolution. *Advances in Colloid and Interface Science* 2021; 294: 102482. doi: 10.1016/J.CIS.2021.102482
95. Zhang L, Forgham H, Shen A, et al. Nanomaterial integrated 3D printing for biomedical applications. *Journal of Materials Chemistry B* 2022; 10(37): 7473–7490. doi: 10.1039/D2TB00931E
96. Kantaros A. 3D printing in regenerative medicine: Technologies and resources utilized. *International Journal of Molecular Sciences* 2022; 23(23): 14621. doi: 10.3390/IJMS232314621
97. Pavan Kalyan BG, Kumar L. 3D printing: Applications in tissue engineering, medical devices, and drug delivery. *AAPS PharmSciTech* 2022; 23(4): 1–20. doi: 10.1208/S12249-022-02242-8
98. Kalkal A, Kumar S, Kumar P, et al. Recent advances in 3D printing technologies for wearable (bio)sensors. *Additive Manufacturing* 2021; 46: 102088. doi: 10.1016/J.ADDMA.2021.102088
99. Bozkurt Y, Karayel E. 3D printing technology; methods, biomedical applications, future opportunities and trends. *Journal of Materials Research and Technology* 2021; 14: 1430–1450. doi: 10.1016/J.JMRT.2021.07.050
100. Wang W, Caetano G, Ambler WS, et al. Enhancing the hydrophilicity and cell attachment of 3D printed PCL/graphene scaffolds for bone tissue engineering. *Materials (Basel)* 2016; 9(12): 992. doi: 10.3390/ma9120992
101. Cheng Z, Landish B, Chi Z, et al. 3D printing hydrogel with graphene oxide is functional in cartilage protection by influencing the signal pathway of Rank/Rankl/OPG. *Materials Science and Engineering: C* 2018; 82: 244–252. doi: 10.1016/j.msec.2017.08.069
102. Chen Q, Mangadlao JD, Wallat J, et al. 3D printing biocompatible polyurethane/poly(lactic acid)/graphene oxide nanocomposites: Anisotropic properties. *ACS Applied Materials & Interfaces* 2017; 9(4): 4015–4023. doi: 10.1021/acsami.6b11793
103. Sayyar S, Bjorninen M, Haimi S, et al. Uv cross-linkable graphene/poly(trimethylene carbonate) composites for 3D printing of electrically conductive scaffolds. *ACS Applied Materials & Interfaces* 2016; 8(46): 31916–31925. doi: 10.1021/acsami.6b09962

Review Article

3D-printed stretchable conductive polymer composites with nano-carbon fillers for multifunctional applications

Chenpeng Zhao†, Ruqing Li†, Biao Fang, Rui Wang, Han Liang, Lei Wang, Ruilin Wu, Yunan Wei, Zhangyuan Wang, Zhipeng Su, Runwei Mo*

School of Mechanical and Power Engineering, East China University of Science and Technology, Shanghai 200231, China

*** Corresponding author:** Runwei Mo, rwmo@ecust.edu.cn

† Chenpeng Zhao and Ruqing Li contributed equally.

Abstract: Carbon nanomaterials are widely used as substrate materials to prepare stretchable conductive composites due to their good stability, strong conductivity, and low price. In response to the demand for optimizing the performance of composite materials, various manufacturing methods for preparing carbon nanomaterial-reinforced stretchable conductive composite materials have emerged. Among them, 3D printing technology has the advantages of flexible processes and excellent product performance and has received widespread attention. This review focuses on the research progress of adding carbon nanomaterials as reinforcing phases to polymer materials using 3D printing technology. The application prospects of conductive polymer composites based on nanocarbon fillers in aerospace, energy storage, biomedicine, and other fields are prospected.

Keywords: carbon-based materials; 3D printing technology; polymer composites; structural design; electronic devices